 doi:10.20944/preprints202210.0249.v1

Article

Integration of Ion Transport Membrane with Conventional Powerplant to Obtain Pure Oxygen and More Efficient Power Production

Arnob Das[1]* and Susmita Datta Peu[2]

[1] Department of Mechanical Engineering, Rajshahi University of Engineering and Technology, Rajshahi-6204, Bangladesh
[2] Department of Agriculture, Hajee Mohammad Danesh Science and Technology University, Dinajpur- 5200, Bangladesh; susmitapeu77@gmail.com
*Corresponding author: arnobarjun@gmail.com or 1602029student.ruet.ac.bd

Abstract: Ion Transport Membrane (ITM) is a well-developed technology for producing O_2 by separating air in its membrane. To decrease energy loss in air separation unit and to increase the overall efficiency of a power generation unit ITM is added with the gasification unit in this model. Ceramic materials are generally used to make ion transport membrane that produces oxygen by conducting oxygen ions at specified temperature. Potential advantages can be gained by integrating ITM technology with power generation units as 99% pure oxygen is produced from ITM. A salient comparison between ITM air separator combined with IGCC and cryogenic air separator combined with IGCC is done in this paper where the total power generation cycle remains same for both cases excluding the air separation units (ITM and cryogenic). Using ITM air separator is more beneficial compared to cryogenic air separation as ITM technology helps to improve IGCC overall efficiency and also reduces plant auxiliaries than that of power generation systems integrated with cryogenic.

Keywords: IGCC; Ion Transport Membrane; air separator; integration; gasifier; HRSG

1. Introduction

The energy demand have been increased with increased population and growth of different power sectors[1] [2]. From the past decades the development of Integrated gasification combined cycle has started and in recent years it is widely used as power generation system. IGCC system has some potential advantages like low amount of sulfur, less NO_X, higher thermal efficiency and higher CO_2 capturing capacity in pre-combustion stage [3]–[6], however, it requires more development and optimization for global utilization [7].

Model of an oxygen-blown IGCC using an Ion Transport Membrane (ITM) to produce oxygen, instead of a conventional cryogenic system. Currently, the most common way to produce oxygen is by cryogenic distillation of air. The process is well-proven, but energy intensive, and expensive to build and operate. Work is underway to develop commercially viable metal-ceramic materials that are selectively permeable to oxygen ions. So-called Ion Transport Membranes are proven at research scales, and are actively being commercialized. Commercial systems promise to produce hundreds to thousands of tons per day of high purity oxygen with significantly lower capital and operating expenses and with lower energy requirements.

This model is derived from (S8-07A) which uses a conventional cryogenic distillation plant for oxygen production. In this model, the ITM is modeled as a black box using the Syngas Separator icon. The fluid type converter is used to make the red streams compatible with the Syngas Separator's inlet and outlet nodes. The other aspects of the model are identical to the original (S8-07A) model.

An article entitled 'ITM Oxygen offers 15% more power and over 10% better plant efficiency' in Gas Turbine World January-February 2008, Volume 38, No. 1 provides some

Preprints (www.preprints.org) | NOT PEER-REVIEWED | Posted: 18 October 2022 doi:10.20944/preprints202210.0249.v1

details about IGCC design using an ITM under development by Air Products and Chemicals. Some of this data was used to prepare this model.

Focusing on the oxygen production portion of the model, air from the GT compressor is pressurized in a boost compressor, and preheated in a recuperator before admission to the topping heater. The air is heated to its final temperature (1088K) by burning syngas before admission to the membrane array. Oxygen ions permeate the selective membrane and form oxygen molecules on the other side. Approximately 90% of the available oxygen is separated from the air when operating around 1088K and GT compressor discharge pressures. The membrane introduces a minor pressure loss. 99% pure oxygen exiting the array is cooled by heating feedwater and then compressed for delivery to the gasifier. Oxygen-depleted air is cooled against O2-rich air in the recuperator and delivered to the GT for NOx reduction and power augmentation. Pressure drops introduced by the recuperator and heat exchangers are overcome by dedicated compressors.

Fuel Specification

Illinois no-6 is used as fuel in this model which is a high volatile bituminous type coal.

Ultimate analysis		Proximate analysis	
	%		%
Moisture	12	Moisture	12
Ash	16	Ash	16
Carbon	55.35	Volatile matter	33
Hydrogen	4	Fixed Carbon	39
Nitrogen	1.08		
Chlorine	0.1		
Sulfur	4		
Oxygen	7.47		
Total	100	Total	100

2. Modeling of the IGCC (Integrated Gasification Combined Cycle) system with ITM (Ion Transport Membrane)

Integrated Gasification Combined Cycle is the system where the syngas produced in gasification chamber is used in a gas turbine to produce electricity[8]. It consists of fuel preparation system, fuel source, cooler (radiant), gas clean-up system, valves, gas turbine system. Here, in this model, IGCC is combined with ITM (ION Transport Membrane) and HRSG (Heat Recovery Steam Generator). To make the power production system more efficient these systems are combined to get the maximum efficiency for power production. In this combined system, ION Transport Membrane is used for oxygen production and this oxygen is supplied in the gasifier where the oxygen mixes with water and fuel and the raw synthesis gas is produced[9]. The temperature of this raw gas is much high and for usability it is moved to the cooler (radiant) where the gas losses some amount of heat and the temperature of the raw gases reduces. Then this raw gas goes through a gas clean-up system where the gas cools down by going through three different coolers and then hydrogen sulfide is removed from the gas. Then this clean syngas is supplied as fuel to the ITM combustor and to the GT system for combustion.

doi:10.20944/preprints202210.0249.v1

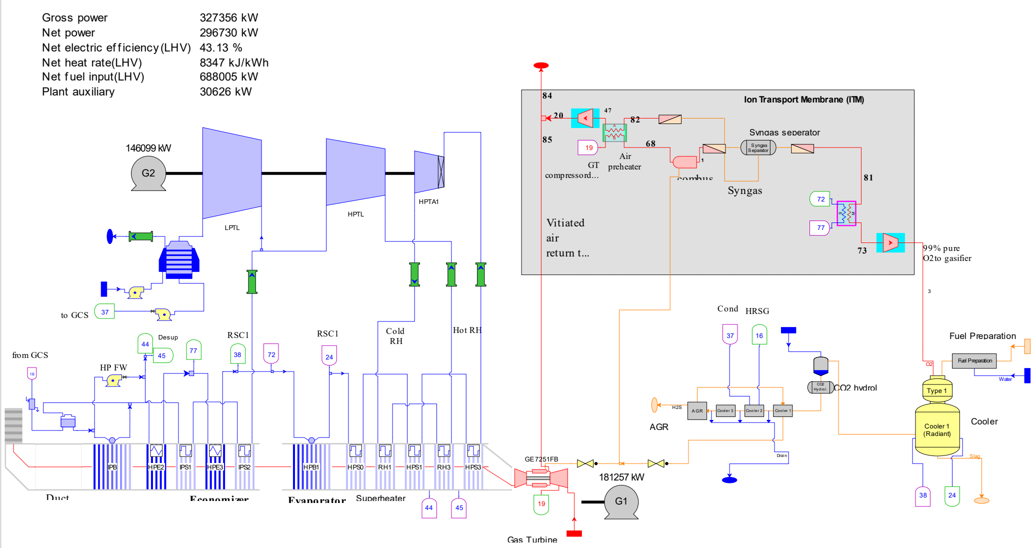

Figure 1. Schematic Diagram of a powerplant consisting ITM, ST, GT, GCS, Reactor.

Air is also supplied to the compressor and mixes with the fuel in the GT combustor. Then the air fuel mixture goes through the turbine and hits the turbine blades for which electricity is produced due to spinning of turbine blades. Then the hot gas from turbine enters HRSG system for the purpose of waste heat treatment and power generation. The processes which are occurred in the HRSG system are discussed briefly in this paper. The hot gas is used to convert water into hot steam by passing the gas through different heating and reheating systems. And the hot steam is used to establish momentum in different turbines by which electricity is produced in the generator connected with turbine shaft.

Synthesis gas (Syngas) production in the gasifier unit:

Gasifier is the chamber where synthesis gas can be produced by gasification of biomass products or other solid waste particles. Gasifier fuel contains high amount of carbon and it's the technology that produces synthesis gas by gasifying carbon containing material like biomass, coal or solid waste[10]. If gasifier fuel contains less amount of fuel then the low-heat value will be less. So, it's better to use such fuel that contains high content of carbon. There is no combustion process involved to convert carbon containing fuels into syngas.

Gasifier wall is maintained very high temperature for gasification of solid waste or biomass. From Table 1 amounts of different elements of fuel can be seen. The gasifier fuel after fuel preparation used in this model contains 16% ash, 12 % moisture, 55.35 % carbon, 4 % hydrogen and other ingredients like nitrogen, sulfur and chlorine in very low amount. The low-heat value of this fuel is 22325 kJ/kg and high heat value is 23491 kJ/kg.

Preprints (www.preprints.org) | NOT PEER-REVIEWED | Posted: 18 October 2022 doi:10.20944/preprints202210.0249.v1

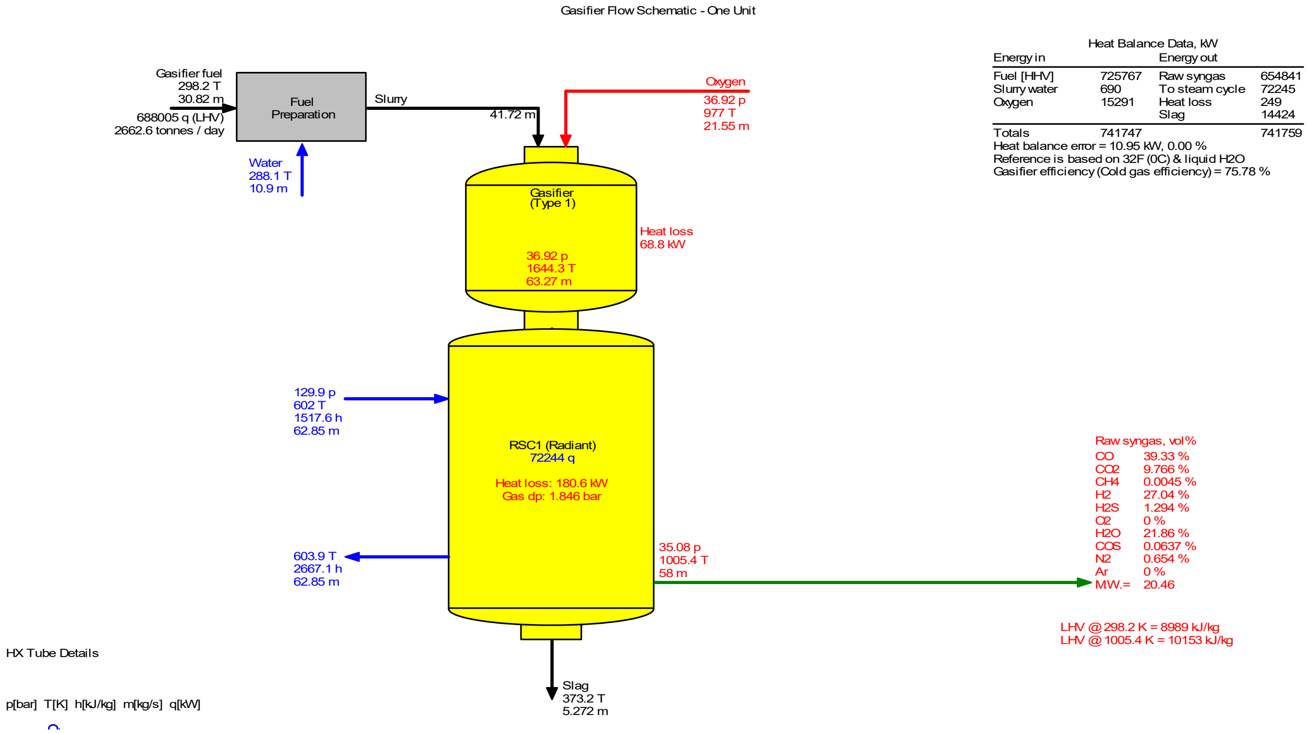

Figure 2. Gasifier Unit.

Before entering the gasifier the fuel is mixed with some amount of slurry water with temperature 288.1 K and pressure 3.447 bar. With the water mixed fuel pure oxygen is also supplied to the gasifier which has a temperature of 977 K and pressure 36.92 bar. The gasification is controlled at very high temperature in the gasifier and the gasifier temperature is maintained at 1644.3 K. Here, the pressure of gasifier is 36.92 bar and nominal fuel flow rate is maintained as 30.82 kg/s. After gasification different gaseous products are produced and of these products, amount of carbon dioxide, hydrogen and water is in top. Here, the efficiency of gasifier is 75.78 % and heat loss in it is accounted as 68.8 kw.

The gasifier is connected with a radiant syngas cooler with water walls where the water wall surface temperature is 678.7 K and heat loss is 180.6 kw. Water enters in this cooler from economizer (HPE3) with temperature 602 K and pressure 129.89 bar. The temperature of hot syngas reduces from 1644.3 K to 1005.4 K and pressure decreases from 36.92 bar to 35.08 bar. There are three exit ways in this cooler. In one way slag is removed at mass flow rate 5.272 kg/s and temperature of slag is 373.2 K and it contains 6.479 % unburnt carbon. In another way water/steam exits the cooler at 603K temperature. And in other way raw syngas exits the cooler with temperature 1005.4 K and pressure 15.08 bar. Then this raw syngas to gas clean-up system where this syngas is treated by different processing to make this gaseous fuel more usable.

Gas clean-up system:

Coming out from gasifier and radiant cooler the raw syngas enters the gas clean up system (GCS) to become more usable[11]. GCS consists of three cooler system, one AGR (acid-gas removal) system and drainage system to remove condensed water[12].

Raw syngas exiting from radiant cooler enters a scrubber which is a part of GCS. Raw syngas enters here with temperature 1005.4 K and pressure 35.08 bar. One water source is added to the scrubber from which water is supplied to cool down the hot raw syngas and after processing in the scrubber temperature of raw syngas decreases to 473.5 K.

Then this raw gas goes through a CO_2 hydrol where hydrolysis of carbonyl sulfide (COS) is occurred and this hydrolysis is an impurity treatment process where hydrolysis of carbonyl sulfide (COS) occurs with present of water to form hydrogen sulfide (H_2S) and

Preprints (www.preprints.org) | NOT PEER-REVIEWED | Posted: 18 October 2022 doi:10.20944/preprints202210.0249.v1

carbon dioxide. Here COS is not corrosive, but H_2S is corrosive. However, COS hydrolysis should be done to get more carbon dioxide to enrich the gaseous fuel.

Reaction: $COS + H_2O \longrightarrow CO_2 + H_2S$

At the time of reaction at CO_2 hydrol, the syngas achieves some heat and the temperature becomes 474.3 K.

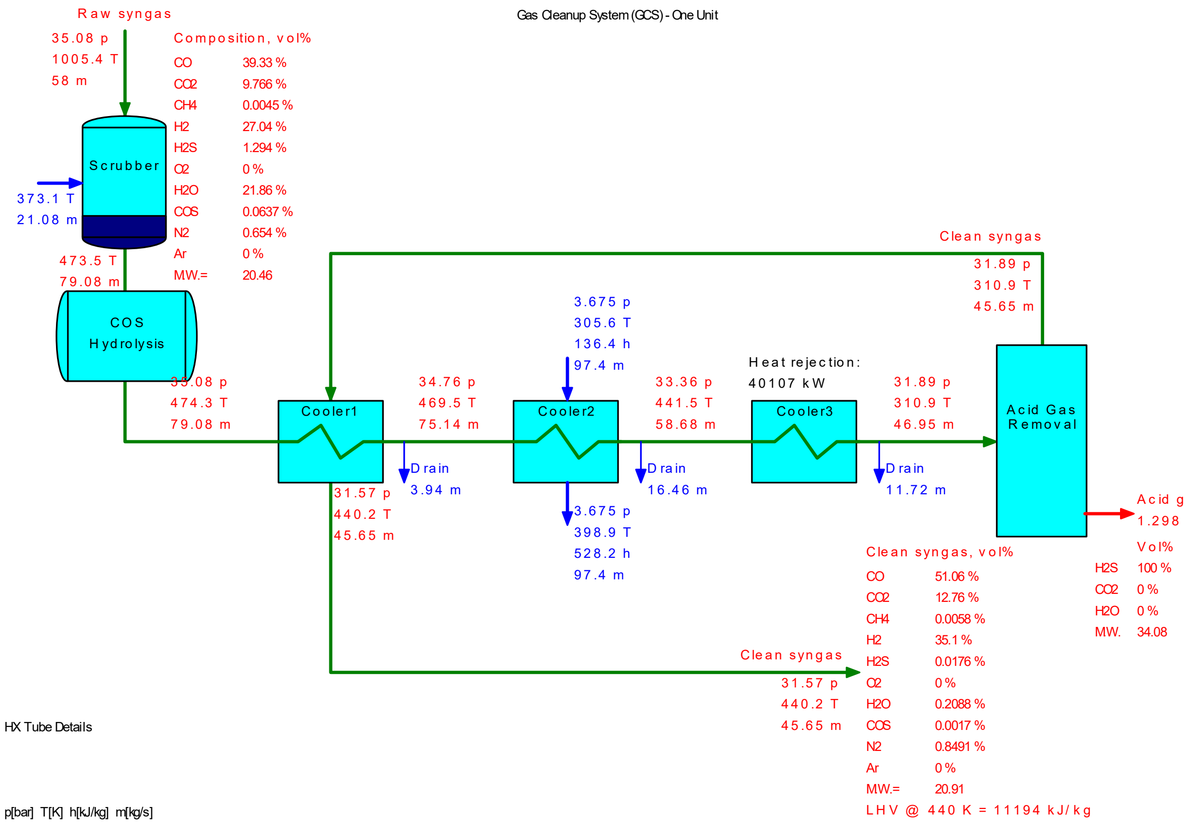

Figure 3. Gas Clean-up system.

Then this syngas enters cooler-1 and its temperature reduces from 474.3 K to 469.5 K. At 3.94 kg/s condensed water is removed from cooler-1 to a drainage system and the amount of heat removal in this cooler is 8651 kw. After this the syngas goes through cooler-2 where condensed water is pumped from water-cooled condenser which is connected to low-pressure turbine (LPTL). This inlet water with temperature 305.6 K exits cooler-2 where the exit water has a temperature 398.9 K after receiving heat from the syngas. At 16.46 kg/s condensed water is removed through the drainage system from cooler-2. After cooling in the syngas exits cooler-2 with temperature 441.5 K and the amount of heat rejection in cooler-2 is accounted as 38156 kw.

Then this cooled syngas enters cooler-3 (external cooler) to become more cooled by releasing heat outside the system and the amount of heat rejection heat is accounted as 40107 kw. Here the syngas temperature decreases from 441.5 K to 310.9 K. At 11.72 kg/s condensed water is removed through the drainage from this system.

After passing external cooler syngas enters an acid-gas removal (AGR) system where the syngas is treated to remove hydrogen sulfide (H_2S). Hydrogen sulfide is an acidic and corrosive ingredient which can cause corrosion of materials of the operating system. So, it's required to remove hydrogen sulfide from syngas to use this syngas as a perfect fuel. Most known and used techniques which are used in AGR are regenerable, cyclic and solvent absorption. There are different types of solvents which are used to remove hydrogen sulfide from syngas by contacting with it in an absorption tower and then the acidic gases are thermally generated in a stripping tower to remove acid gases (H_2S). The most common solvents which are used in AGR system are shown in table-1.

Table 1. Common solvents used in Acid-Gas Removal system.

Solvent type		Working procedure	Example of solvent
1.	Chemical solvent	These are aqueous based which reacts with hydrogen sulfide reversibly after hydrolyzing in water to weak acids	Methanolamine (MEA), methyl-diethanolamine (MDEA) [13]
2.	Physical solvent	These are polar molecules having negative and positive charge which attract the polar hydrogen sulfide. Here absorption is performed at low temperature and it also requires cooling.	Selexol, rectisol, purisol, morphysorb [14]
3.	Chemical-physical/mixed solvent	This process includes both the chemical solvents and physical solvents and it also requires cooling	Sulfinol, amisol [15]
4.	Oxidative solvent	These solvents are used to oxidize hydrogen sulfide to elemental sulfur reacting with it where the sulfur is recovered as a solid.	Sulferox, Lo-Cat [16]

Using AGR system 100% hydrogen sulfide is removed from the synthesis gas and the raw syngas is cleaned by processing in AGR. This clean syngas exits AGR with temperature 310.9 K and enters syngas reheater (cooler-1) where it gains some heat from the coming raw syngas and the exit temperature of clean syngas is 440.2 K. Carbon dioxide and hydrogen are the high amount ingredients of the clean syngas coming out from the gas clean-up system and this clean syngas exit GCS at 45.65 kg/s mass flow rate.

Gas turbine:

Air enters in the compressor from an air source and also from the air compressor which is connected with the ITM unit. Air enters from an air source with 288.2 K temperature and 1.013 bar pressure and air from ITM air compressor enters with temperature 971.4 K and pressure 18.74 bar. At first, fuel coming out from gas clean up system enters in a valve where pressure drop occurs 1.579 bar and then divided into two ways in a splitter. In one way some amount of clean syngas enters ITM combustor and in another way the remaining part of clean syngas enters in the gas turbine system for burning to achieve high temperature. Clean syngas enters the GT system with a temperature 440.2 K and pressure 18.74 bar. Air is discharged from the GT compressor at temperature 674.4 K and pressure 17.67 bar which goes through ITM air preheater. Here the efficiency of GT for low-heat-value is 38.49 % and for high-heat-value it is 36.05 %. Exhaust air from the turbine exits at temperature 912.6 K and pressure 1.0379 bar and then enters in the HRSG (Heat Recovery Steam Generator) system. The turbine is connected with the generator through a shaft where mechanical power is supplied by the turbine shaft.

Here some values are listed in the table-2.

Table 2. Input and output power in different sources.

Generator power output	181257 kw
Shaft power	183830 kw
Compressor power	174901 kw
Turbine power	359875 kw
Mechanical loss	1143.2 kw
Generator loss	2573.2 kw

Emissions from Gas Turbine:

Sulfur dioxide is emitted at a rate 91.1 kg/hr and per year the amount of SO_2 emission is 798 metric tons. Net carbon dioxide is emitted 207316 kg/hr and per year the amount of CO_2 emission is 1816088 metric tons.

Heat Recovery Steam Generator

Water comes out from cooler-2 of Gas-Cleanup-System and enters the make-up/blowdown and after processing the make-up water exits from make-up system. This make-up water and the heating steam splitting out from evaporator (IPB) enter into the deaerator. The type of deaerator which is used in this model is horizontal heater. Here the operating pressure is 3.675 bar, operating temperature 413.7 K and total storage volume is 45773 L. The feed water exits deaerator at a mass flow rate of 100.8 kg/s, temperature 413.7 K and pressure 3,675 bar.

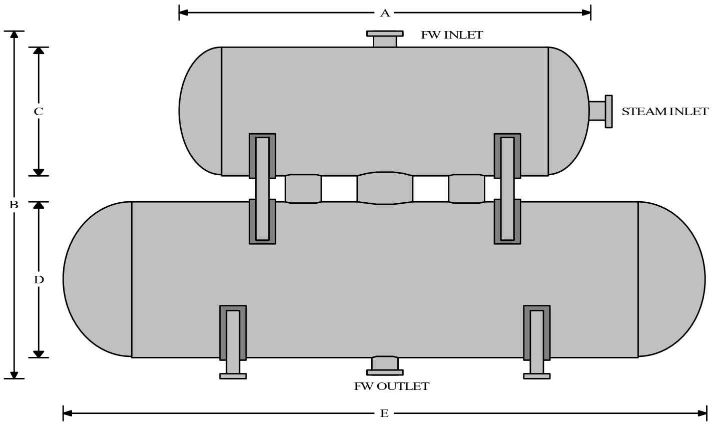

Figure 4. Elevation view of deaerator.

This feedwater split into two parts in the splitter. Some amount of feed water goes through evaporator (IPB) and the other amount goes through a pump (24). In the evaporator (IPB) the enthalpy of steam increases and the exit steam from evaporator goes through a splitter from where some amount of steam goes again towards deaerator and another amount from splitter enters superheater (IPS1). In this superheater, mass flow rate of entering and exiting steam is 4.97 kg/s and temperature rises from 413 K to 533 K. This superheated steam exiting from superheater (IPS1) enters the superheater (IPS2). Here, the superheated steam gains more heat and rises its temperature from 533 K to 593 K and the mass flow rate of steam is same as before 4.97 kg/s. Then the superheated steam coming out from superheater (IPS2) goes through a pipe (22) and then mixes with the steam exiting from high pressure turbine (HPTL) in a mixer (18). Then this mixed hot steam enters low pressure turbine (LPTL).

The remaining amount of split feed water exiting from the deaerator enters a multi-stage centrifugal pump which is driven by an integral motor and this pump consume 2422 KW electricity. Feed water exiting from the pump enters a splitter and divided into two ways. Some amount of feed water goes through superheater RH3 and HPS3 and the other remaining amount enters economizer HPE2. In this economizer, the inlet temperature of water is 417 K and the exit temperature is 538 K. Water exiting from economizer (HPE2) enters in a splitter where it splitted into two ways. In one way some amount of water enters into a heat exchanger (53) to cool the incoming gas and in another way the remaining amount of water enters an economizer (HPE3) where the temperature of water increases from 538 to 602 K. The exiting water enters a splitter and some amount of splitted water enters the cooler 1 (radiant) and the remaining amount of water mixes with the exit water from heat exchanger (53) in a mixer (54) and then the mixed water enters an evaporator (HPB1). Here in this evaporator the inlet water is converted into steam. Steam after

Preprints (www.preprints.org) | NOT PEER-REVIEWED | Posted: 18 October 2022 doi:10.20944/preprints202210.0249.v1

leaving evaporator mixes with the exit steam coming from the cooler 1 (radiant) in a mixer and then this mixed steam enters a superheater (HPS0). In this superheater the inlet steam temperature is 603.9 K and the exit temperature of steam is 740.4 K. Then the superheated steam goes to another superheater (HPS1) and the steam temperature increases from 740.4 to 800.4 K. Then this superheated steam goes through superheater HPS3 and the steam temperature increases from 800.4 K to 840.4 K. Some amount of feed water is supplied before from the deaerator. This superheated steam goes through a pipe (19) and enters in the high-pressure turbine (HPTA1) and give momentum to turbine blades to rotate. In this turbine, the overall efficiency is 87.31%, expansion power is 34016 KW, shaft power is 33912 kw and mechanical loss is 103.9 KW and the inlet and outlet temperature are 838.9 K and 633.9 K respectively. Here, high pressure end leakages are 0.2929 kg/s and 1.483 kg/s and the low-pressure leakage is 0.5784 kg/s. As expansion occurs in the turbine so both the pressure and temperature decrease and inlet and outlet pressure in this turbine are 124.1 bar and 30.97 bar respectively.

The outlet steam of turbine HPTA1 enters into a superheater (RH1) with steam temperature 631.8 K and pressure 29.81. After heating the superheated steam exits the superheater with temperature 780.3 K and pressure 28.82 bar. Here, the heat transfer rate from gas is 30370 kw and heat transfer rate to water is 30219 kw and so in this superheater heat loss is 151.2 kw.

Then the superheated steam coming out from superheater RH1 enters a superheater (RH3) and after heating the temperature rises from 780.3 K to 840.3 K. Here the amount of heat loss is 60.96 kw. The superheated steam enters a high-pressure turbine (HPTL) through a pipe. As expansion occurs so the volume increases and the temperature and pressure reduce for the turbine work. In this turbine, Pressure decreases from 26.81 bar to 3.447 bar, temperature decreases from 838.7 K to 563.5 K and enthalpy also reduces. Here, group overall efficiency for this turbine is 88.38%, expansion power 51031 kw, shaft power is 50875 kw and mechanical loss is 155.8 kw. High-pressure end leakage in is accounted as 1.718 kg/s. The exit steam of turbine HPTL mixes with the steam coming from superheater IPS2 in a mixer and then enters into a low-pressure turbine. Here for expansion temperature decreases from 565 K to 303.4 K and pressure decreases from 3.447 bar to 0.0483 bar. Expansion power of this turbine is 63487, shaft power is 63293 kw and mechanical loss 193.93 kw. Group overall efficiency of this turbine is 89.11 % and low-pressure leakage in 0.5526 kg/s.

Annulus velocity is 219.8 m/s and for this exhaust loss is accounted as 26.62 kJ/kg. From the graph shown in figure- relation between annulus velocity and exhaust loss can be realized.

Preprints (www.preprints.org) | NOT PEER-REVIEWED | Posted: 18 October 2022 doi:10.20944/preprints202210.0249.v1

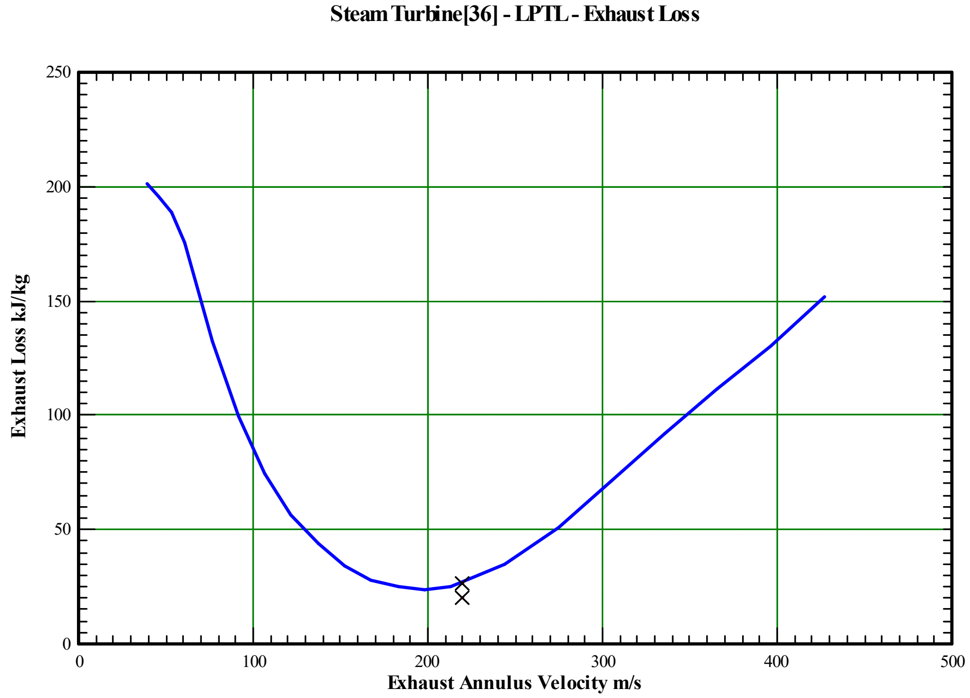

Figure 5. Relationship between exhaust velocity and exhaust loss.

With the processing of these turbines (HPTA1, HPTL, LPTL) the generator gets power to produce electricity. The generator is driven by these three turbines. The total shaft power of these three turbines equals to 148080 kw which is the final shaft power goes to generator to convert mechanical power to electricity and the shaft speed is 3600 rpm. Here, the generator nameplate power is 153404 kw and nameplate efficiency 98.68 %. But the generator power output is 146099 kw and generator efficiency 98.66 %. Total generator loss is accounted as 1981.5 kw which is contributed by 1738.5 kw of electrical loss and 243 kw of mechanical loss.

The exit steam from low-pressure turbine (LPTL) enters in a water-cooled condenser and some amount of cooling water is pumped in this condenser from a water source. The pump type is vertical turbine driven by an integral motor and it's mechanical and isentropic efficiency is 97% and 87% respectively. After cooling and condensation some amount of water is carried out through a pipe in a water sink and the remaining amount of water is pumped to cooler 2 of gas clean-up system.

Ion Transport Membrane (ITM) unit

Ion Transport Membrane is a recently developed technology to produce pure oxygen from syngas[17]. There are different companies of developed countries which are working to develop ceramic membranes for the purpose of oxygen separation from hot air. Different air products and various chemicals are used to develop an ion transport membrane system. Ion transport membrane system is based on ceramic membranes which operate at very high temperature to produce oxygen. These membranes carry out the separation of oxygen from air of very high temperature like 900-1100 K. There is no requirement of any electrodes or any electrical circuit to operate in the ion transport membrane system.

The O2 diffuses from the high oxygen partial pressure side towards the low oxygen partial pressure side, maintaining overall charge neutrality via counterbalancing electron flux. The air is heated to its final temperature (1088K) by burning syngas before admission to the membrane array. Oxygen ions permeate the selective membrane and form oxygen

 doi:10.20944/preprints202210.0249.v1

molecules on the other side. Approximately 90% of the available oxygen is separated from the air when operating around 1088K and GT compressor discharge pressures.

In the combustor, air is burnt at very high temperature (900-1100 K) and clean syngas is used as fuel to burn the air. Air from gas turbine compressor enters into an air compressor with temperature 674.5 K and pressure 17.67 bar. The exit temperature and pressure from this air compressor are 869.5 K and 15.369 bar. This hot air then goes to a combustor to become more heated by burning gaseous fuel which exits form gas clean up system and then coming through valve and splitter. This gaseous fuel enters the combustor with temperature 440.2 K and pressure 16.91 bar.

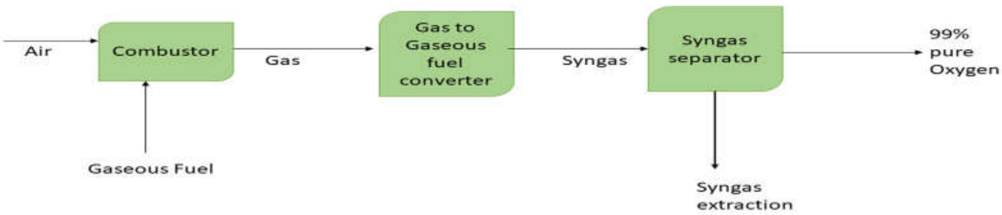

Figure 6. Schematic diagram of Ion Transport Membrane Unit.

After burning in the combustor the air achieves a temperature of 1088.7 K. Combustion is controlled by the specified outlet temperature. Fuel inlet at low heat value is 30641 kw, at high heat value 32715 kw and combustor heat loss is 92.66 kw. Then the hot gas enters in a converter and here the hot gas is converted into gaseous fuel and then goes the o syngas separator. In this separator, syngas is separated into two portions. In one exit way, oxygen-rich rich gas is exited where the amount of oxygen is 99%, nitrogen 0.9943 % and sulfur dioxide 0.0038 %. In another way the syngas is extracted from the syngas separator where the amount of nitrogen is 91.33 %, carbon dioxide 2.649 %oxygen 2.278 % and argon 1.102 %. This extraction syngas is in gaseous fuel form with much high temperature and this gaseous fuel is converted into air in a converter. Then this hot air (1088.7 K) enters an air preheater and its temperature reduces at 866.5 K by releasing heat to the incoming air coming from GT compressor. Then this gas with temperature 866.5 K goes through an gas/air compressor where its temperature increases at 971.4 K and pressure increases from 12.47 bar to 18.74 bar. Here the compression power is 11287 kw, shaft power 11309 kw, mechanical loss 22.62 kw and mechanical efficiency of this compressor is 99.8 %.

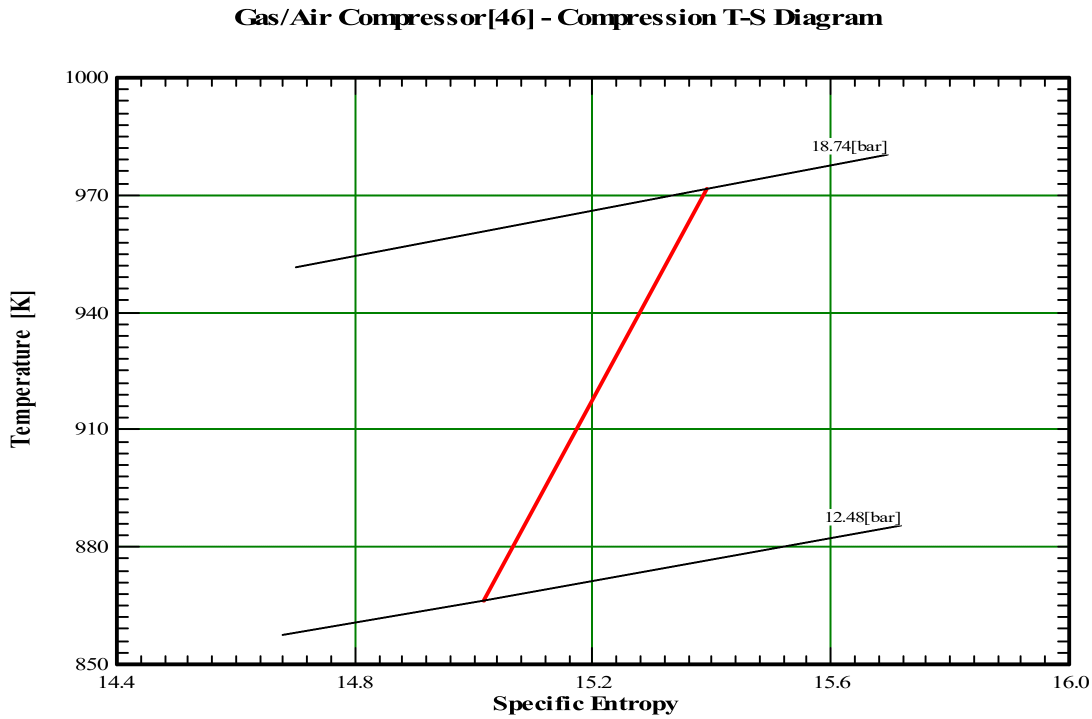

Figure 7. T-S diagram for Gas/Air compressor (46).

From the T-S diagram shown in figure- the change of properties of air can be realized. Then the compressed gas goes through a splitter where it divides in two ways. In one way some amount of gas is rejected in a gas sink and remaining amount of gas enters gas turbine compressor with temperature 971.4 K and pressure 18.74 bar.

Table 3. Fuel properties in different places of the system.

Fuel Streams: Additional Properties			
Stream 2 - Outlet of Fuel Fluid Type Converter [12] -> Syngas inlet of Syngas Separator [57] 'Gaseous fuel defined by mole percent'			
Oxygen	O2	18.87	%
Water Vapor	H_2O	2.188	%
Nitrogen	N2	75.83	%
Carbon Dioxide	CO2	2.195	%
Sulfur Dioxide	SO2	0.0007	%
Argon	Ar	0.9129	%
LHV		0	kJ/kg
HHV		33.19	kJ/kg
Molecular Weight		29.01	
Stream 13 - Outlet of Fuel Source [9] -> Fuel inlet of Gasifier (Type 1, One-Stage Slurry) [14] 'Solid fuel defined by weight percent'			
Weight percent of Ash		16	%
Weight percent of Moisture		12	%
Weight percent of Carbon		55.35	%

Preprints (www.preprints.org) | NOT PEER-REVIEWED | Posted: 18 October 2022 doi:10.20944/preprints202210.0249.v1

Weight percent of Hydrogen		4	%
Weight percent of Oxygen		7.47	%
Weight percent of Nitrogen		1.08	%
Weight percent of Sulfur		4	%
Weight percent of Chlorine		0.1	%
LHV		22325	kJ/kg
HHV		23491	kJ/kg
Stream 14 - Clean syngas outlet of Gas Cleanup System (Legacy) [10] -> Inlet of Valve [44] 'Gaseous fuel defined by mole percent'			
Hydrogen	H2	35.1	%
Water Vapor	H2O	0.2088	%
Nitrogen	N2	0.8491	%
Carbon Monoxide	CO	51.06	%
Carbon Dioxide	CO2	12.76	%
Methane	CH4	0.0058	%
Hydrogen Sulfide	H2S	0.0176	%
Carbonyl Sulfide	COS	0.0017	%
LHV		10986	kJ/kg
HHV		11730	kJ/kg
Molecular Weight		20.91	
Stream 17 - Acid gas outlet of Gas Cleanup System (Legacy) [10] -> Inlet of Fuel Sink [8] 'Gaseous fuel defined by mole percent'			
Hydrogen Sulfide	H2S	100	%
LHV		15204	kJ/kg
HHV		16495	kJ/kg
Molecular Weight		34.08	
Stream 22 - Raw syngas outlet of Gasifier (Type 1, One-Stage Slurry) [14] -> Raw syngas inlet of Gas Cleanup System (Legacy) [10] 'Gaseous fuel defined by mole percent'			
Hydrogen	H2	27.04	%
Water Vapor	H2O	21.86	%
Nitrogen	N2	0.654	%
Carbon Monoxide	CO	39.33	%
Carbon Dioxide	CO2	9.766	%
Methane	CH4	0.0045	%
Hydrogen Sulfide	H2S	1.294	%
Carbonyl Sufide	COS	0.0637	%
LHV		8989	kJ/kg
HHV		10069	kJ/kg

Preprints (www.preprints.org) | NOT PEER-REVIEWED | Posted: 18 October 2022 doi:10.20944/preprints202210.0249.v1

Molecular Weight		20.46	
Stream 23 - Slag outlet of Gasifier (Type 1, One-Stage Slurry) [14] -> Inlet of Fuel Sink [7] 'Solid fuel defined by weight percent'			
Weight percent of Ash		93.52	%
Weight percent of Moisture		0	%
Weight percent of Carbon		6.379	%
Weight percent of Hydrogen		0	%
Weight percent of Oxygen		0	%
Weight percent of Nitrogen		0	%
Weight percent of Sulfur		0	%
Weight percent of Chlorine		0.1	%
LHV		2121.2	kJ/kg
HHV		2121.2	kJ/kg
Stream 65 - Outlet of Valve [44] -> Inlet of Splitter [55] 'Gaseous fuel defined by mole percent'			
Hydrogen	H2	35.1	%
Water Vapor	H2O	0.2088	%
Nitrogen	N2	0.8491	%
Carbon Monoxide	CO	51.06	%
Carbon Dioxide	CO2	12.76	%
Methane	CH4	0.0058	%
Hydrogen Sulfide	H2S	0.0176	%
Carbonyl Sufide	COS	0.0017	%
LHV		10986	kJ/kg
HHV		11730	kJ/kg
Molecular Weight		20.91	
Stream 75 - Outlet 2 of Splitter [55] -> Inlet of Valve [60] 'Gaseous fuel defined by mole percent'			
Hydrogen	H2	35.1	%
Water Vapor	H2O	0.2088	%
Nitrogen	N2	0.8491	%
Carbon Monoxide	CO	51.06	%
Carbon Dioxide	CO2	12.76	%
Methane	CH4	0.0058	%
Hydrogen Sulfide	H2S	0.0176	%
Carbonyl Sufide	COS	0.0017	%
LHV		10986	kJ/kg
HHV		11730	kJ/kg
Molecular Weight		20.91	

Preprints (www.preprints.org) | NOT PEER-REVIEWED | Posted: 18 October 2022 doi:10.20944/preprints202210.0249.v1

Stream 76 - Outlet of Valve [60] -> Fuel inlet of Gas Turbine (GT PRO) [11] 'Gaseous fuel defined by mole percent'			
Hydrogen	H2	35.1	%
Water Vapor	H2O	0.2088	%
Nitrogen	N2	0.8491	%
Carbon Monoxide	CO	51.06	%
Carbon Dioxide	CO2	12.76	%
Methane	CH4	0.0058	%
Hydrogen Sulfide	H2S	0.0176	%
Carbonyl Sufide	COS	0.0017	%
LHV		10986	kJ/kg
HHV		11730	kJ/kg
Molecular Weight		20.91	
Stream 79 - Main syngas outlet of Syngas Separator [57] -> Inlet of Gas/Air Fluid Type Converter [58] 'Gaseous fuel defined by mole percent'			
Oxygen	O2	99	%
Nitrogen	N2	0.9943	%
Sulfur Dioxide	SO2	0.0038	%
LHV		0	kJ/kg
HHV		0	kJ/kg
Molecular Weight		31.96	
Stream 80 - Syngas extraction outlet of Syngas Separator [57] -> Inlet of Gas/Air Fluid Type Converter [59] 'Gaseous fuel defined by mole percent'			
Oxygen	O2	2.278	%
Water Vapor	H2O	2.642	%
Nitrogen	N2	91.33	%
Carbon Dioxide	CO2	2.649	%
Argon	Ar	1.102	%
LHV		0	kJ/kg
HHV		40.93	kJ/kg
Molecular Weight		28.4	
Stream 83 - Outlet 3 of Splitter [55] -> Fuel inlet of Combustor [1] - combustor 'Gaseous fuel defined by mole percent'			
Hydrogen	H2	35.1	%
Water Vapor	H2O	0.2088	%
Nitrogen	N2	0.8491	%
Carbon Monoxide	CO	51.06	%
Carbon Dioxide	CO2	12.76	%
Methane	CH4	0.0058	%
Hydrogen Sulfide	H2S	0.0176	%

Preprints (www.preprints.org) | NOT PEER-REVIEWED | Posted: 18 October 2022 doi:10.20944/preprints202210.0249.v1

Carbonyl Sufide	COS	0.0017	%
LHV		10986	kJ/kg
HHV		11730	kJ/kg
Molecular Weight		20.91	

Gas/Air - 26 Streams														
H* is fluid enthalpy referenced to zero at 77F (25C) with H2O as vapor														
Gas/Air Psychrometric Properties only for T <= 500 F/260 C														
No. [Name]	**P**	**T**	**H***	**Mgas**	**Mash**	**V**	**M.W.**	**Mole Composition %**						
	[bar]	**[K]**	**[kJ/kg]**	**[kg/s]**	**[kg/s]**	**[m^3/s]**		**N_2**	**O_2**	**CO_2**	**H_2Ov**	**H_2Ol**	**Ar**	**SO_2**
1	14.778	1088.71	863.17	114.1	0	24.1	29.009	75.829	18.875	2.195	2.188	0	0.913	0.001
3	36.92	977.04	686.63	21.55	0	1.5	31.962	0.994	99.002	0	0	0	0	0.004
5	1.0197	566.67	282.84	464.5	0	731.4	29.343	74.594	9.825	8.833	5.848	0	0.897	0.002
7	1.0162	462.09	170.76	464.5	0	598.4	29.343	74.594	9.825	8.833	5.848	0	0.897	0.002
9	1.023	617.25	338.09	464.5	0	794.1	29.343	74.594	9.825	8.833	5.848	0	0.897	0.002
11	1.0151	427.07	133.84	464.5	0	553.7	29.343	74.594	9.824	8.833	5.848	0	0.897	0.002
18	1.0329	911.45	673.72	464.5	0	1161.3	29.343	74.593	9.826	8.833	5.848	0	0.897	0.002
19	17.67	674.5	390.48	111.3	0	12.2	28.856	77.292	20.738	0.03	1.009	0	0.931	0
20	18.74	971.42	737.36	92.5	0	14	28.397	91.329	2.278	2.649	2.642	0	1.102	0
21	1.0132	288.15	-10.13	440.4	0	360.9	28.856	77.292	20.738	0.03	1.009	0	0.931	0
25	1.0379	912.56	675.03	464.5	0	1157.2	29.343	74.593	9.826	8.833	5.848	0	0.897	0.002
47	12.476	866.48	615.34	92.5	0	18.8	28.397	91.329	2.278	2.649	2.642	0	1.102	0
51	1.0324	893.64	652.74	464.5	0	1139.3	29.343	74.593	9.826	8.833	5.848	0	0.897	0.002
53	1.0312	871.15	626.36	464.5	0	1111.8	29.343	74.593	9.826	8.833	5.848	0	0.897	0.002

Preprints (www.preprints.org) | NOT PEER-REVIEWED | Posted: 18 October 2022 doi:10.20944/preprints202210.0249.v1

55	1.0306	842.73	593.22	464.5	0	1076.2	29.343	74.593	9.826	8.833	5.848	0	0.897	0.002
57	1.0287	786.12	527.84	464.5	0	1005.8	29.343	74.593	9.826	8.833	5.848	0	0.897	0.002
59	1.0255	683.58	411.66	464.5	0	877.3	29.343	74.593	9.825	8.833	5.848	0	0.897	0.002
61	1.023	616.05	336.78	464.5	0	792.6	29.343	74.594	9.825	8.833	5.848	0	0.897	0.002
63	1.0196	564.16	280.12	464.5	0	728.2	29.343	74.594	9.825	8.833	5.848	0	0.897	0.002
68	15.369	869.54	605.07	111.3	0	18.1	28.856	77.292	20.738	0.03	1.009	0	0.931	0
73	12.476	727.59	419.87	21.55	0	3.3	31.962	0.994	99.002	0	0	0	0	0.004
81	14.347	1088.71	808.59	21.55	0	4.3	31.962	0.994	99.002	0	0	0	0	0.004
82	14.347	1088.71	876.07	92.5	0	20.6	28.397	91.329	2.278	2.649	2.642	0	1.102	0
84	1.0132	972.1	737.36	0.009	0	0	28.397	91.329	2.278	2.649	2.642	0	1.102	0
85	18.74	971.42	737.36	92.49	0	14	28.397	91.329	2.278	2.649	2.642	0	1.102	0
94	1.0151	427.07	133.84	464.5	0	553.7	29.343	74.594	9.824	8.833	5.848	0	0.897	0.002

Gas/Air Psychrometric Properties (T <= 500 F/260 C)

No. [Name]	P	T	Dew Point	Wet Bulb	Sulfur Dew Point	RH
	[bar]	[K]	[K]	[K]	[K]	[%]
7	1.0162	462.09	309.16	326.33	385.23	0.48
11	1.0151	427.07	309.14	323.41	385.21	1.12
21	1.0132	288.15	280.44	283.97		60
94	1.0151	427.07	309.14	323.41	385.21	1.12

Water/Steam - 48 Streams

Steam Property Formulation - IFC-67

H* is fluid enthalpy referenced to zero at 77F (25C) with H2O as vapor

H is enthalpy referenced to zero at 32F (0C) with H2O as liquid

No. [Name]	P	T	H*	H	M	Quality	Sup/Sub(-).
	[bar]	[K]	[kJ/kg]	[kJ/kg]	[kg/s]		[K]

4	3.675	413.75	-1955.86	591.63	100.8	0	
6	129.89	601.98	-1029.87	1517.62	69.85		-1.9
8	149.37	538.66	-1386.81	1160.68	92.81		-76.3
10	129.89	603.91	119.58	2667.07	29.66		0
12	3.675	413.75	-1955.86	591.63	8.042	0	
15	31.57	397.69	-2022.47	525.02	32.12		-112.1
16	3.675	398.89	-2019.29	528.2	97.4		-14.9
24	129.89	603.91	119.58	2667.07	62.85		0
26	3.675	398.38	-2021.44	526.04	97.86		-15.4
27	129.89	603.91	119.58	2667.07	92.51		0
28	3.447	564.98	504.18	3051.67	96.84		153.5
29	124.1	838.88	967.83	3515.32	92.51		238.5
30	29.8	631.77	590.44	3137.93	90.16		125.2
31	26.81	838.72	1058.35	3605.83	90.16		337.9
32	3.447	591.85	559.12	3106.61	4.97		180.4
33	1.0132	298.17	-2442.56	104.93	5282.3		-75
34	151.58	417.22	-1931.42	616.07	92.81		-198.9
35	3.675	413.75	-1955.86	591.63	92.81	0	
36	2.499	288.16	-2484.28	63.21	5282.3		-112.4
37	3.675	305.65	-2411.06	136.43	97.4		-108.1
38	129.89	601.98	-1029.87	1517.62	62.85		-1.9
39	129.89	601.98	-1029.87	1517.62	7.001		-1.9
40	3.675	413.75	186.16	2733.65	2.992	1	
41	3.675	413.75	186.16	2733.65	4.97	1	
42	151.58	417.22	-1931.42	616.07	0		-198.9
43	151.58	417.22	-1931.42	616.07	92.81		-198.9
44	28.82	419.07	-1931.42	616.07	0		-85.7
45	151.58	417.22	-1931.42	616.07	0		-198.9
46	3.675	413.75	186.16	2733.65	7.963	1	
48	30.97	633.87	592.94	3140.43	90.16		125.1
49	3.447	563.52	501.21	3048.7	91.87		152
50	0.0483	305.42	-149.23	2398.26	97.4	0.9332	
52	125.5	840.39	970.33	3517.82	92.51		239.2
54	27.85	840.25	1060.85	3608.33	90.16		337.4
56	126.96	800.39	865.53	3413.02	92.51		198.3
58	28.82	780.25	925.62	3473.1	90.16		275.5
60	128.42	740.38	699.96	3247.45	92.51		137.4
62	3.534	593.16	561.62	3109.11	4.97		180.8
64	3.604	533.51	439.41	2986.9	4.97		120.5
66	0.4072	305.41	-2412.35	135.14	97.4		-44.1
67	1.522	298.16	-2442.56	104.93	5282.3		-86.8

69	3.447	288.15	-2484.22	63.27	10.9		-123.3
70	35.08	373.15	-2125.9	421.59	21.08		-142.7
71	1.0132	288.15	-2484.46	63.03	5282.3		-85
72	129.89	602.6	-1025.5	1521.99	22.95		-1.3
74	129.89	602.45	-1026.52	1520.97	29.96		-1.5
77	149.37	538.66	-1386.81	1160.68	22.95		-76.3
78	131.84	538.62	-1386.81	1160.68	69.85		-66.4

3. Results and Discussion

Table 4. Comparison of plant auxiliaries for ITM ASU and Cryogenic auxiliaries.

Plant Summary		ITM ASU	Cryogenic ASU
Ambient pressure	bar	1.013	14.7
Ambient temperature	K	288.1	59
Ambient RH	%	60	60
Ambient wet bulb temperature	K	284	51.48
Gross power	kW	327356	326024
Gross electric efficiency(LHV)	%	47.58	45.25
Gross heat rate(LHV)	kJ/kWh	7566	7541
Net power	kW	296730	280622
Net electric efficiency(LHV)	%	43.13	38.95
Net heat rate(LHV)	kJ/kWh	8347	8761
Net fuel input(LHV)	kW	688005	2458513
Net process heat output	kW	0	0
CHP efficiency	%	43.13	38.95
PURPA efficiency	%	43.13	38.95
Plant auxiliary	kW	30626	45402
Net electric efficiency(HHV)	%	40.99	37.02
Net heat rate(HHV)	kJ/kWh	8783	9219
Net fuel input(HHV)	kW	723942	2586931
Energy chargeable to power	kW	688005	2458513
Electric efficiency on chargeable energy	%	43.13	38.95

4. Conclusion

Power consumption rate is reduced for the auxiliary components which is possible due to larger amount of air extraction rate. The air compressor consumes less amount of power which causes increase in net efficiency of system and this increase in net efficiency is very low because of the loss of ai mass flow rate from GT combustor. Comparing with cryogenic air separator the ITM system has capacity to increase net power production and improve net efficiency by reducing auxiliary load with a small incremental fuel demand. In this particular case, the gross power increased by about 1MW out of 326MW, while the auxiliary load was reduced from 44.8 to 30.3MW resulting in 15.5MW increase in net power. However, some additional fuel is burnt to heat the air for the ITM, so the fuel consumption increases. Nonetheless, LHV net electric efficiency improves from about 39% in the base (cryogenic ASU) case to about 43% in this case, a noteworthy increase.

References

1. A. Das and S. D. Peu, "A Comprehensive Review on Recent Advancements in Thermochemical Processes for Clean Hydrogen Production to Decarbonize the Energy Sector," *Sustainability 2022, Vol. 14, Page 11206*, vol. 14, no. 18, p. 11206, Sep. 2022, doi: 10.3390/SU141811206.

2. A. Das and S. Peu, "Modeling of PV Cell, PV Module, PV Array and PV IV Characteristics Analysis Using MATLAB/SIMULINK," Sep. 2022, doi: 10.20944/PREPRINTS202209.0304.V1.
3. P. Mahapatra and B. W. Bequette, "Design and Control of an Elevated-Pressure Air Separations Unit for IGCC Power Plants in a Process Simulator Environment," *Ind Eng Chem Res*, vol. 52, no. 9, pp. 3178–3191, Mar. 2012, doi: 10.1021/IE301034E.
4. H. Liu, W. Ni, Z. Li, and L. Ma, "Strategic thinking on IGCC development in China," *Energy Policy*, vol. 36, no. 1, pp. 1–11, Jan. 2008, doi: 10.1016/J.ENPOL.2007.08.034.
5. C. Descamps, C. Bouallou, and M. Kanniche, "Efficiency of an Integrated Gasification Combined Cycle (IGCC) power plant including CO2 removal," *Energy*, vol. 33, no. 6, pp. 874–881, Jun. 2008, doi: 10.1016/J.ENERGY.2007.07.013.
6. J. Zhang, Z. Zhou, L. Ma, Z. Li, and W. Ni, "Efficiency of wet feed IGCC (integrated gasification combined cycle) systems with coal–water slurry preheating vaporization technology," *Energy*, vol. 51, pp. 137–145, Mar. 2013, doi: 10.1016/J.ENERGY.2012.12.024.
7. L. Han *et al.*, "Simulation and optimization of ion transfer membrane air separation unit in an IGCC power plant," *Appl Therm Eng*, vol. 129, pp. 1478–1487, Jan. 2018, doi: 10.1016/J.APPLTHERMALENG.2017.10.131.
8. C. Descamps, C. Bouallou, and M. Kanniche, "Efficiency of an Integrated Gasification Combined Cycle (IGCC) power plant including CO2 removal," *Energy*, vol. 33, no. 6, pp. 874–881, Jun. 2008, doi: 10.1016/J.ENERGY.2007.07.013.
9. P. N. Dyer, R. E. Richards, S. L. Russek, and D. M. Taylor, "Ion transport membrane technology for oxygen separation and syngas production," *Solid State Ion*, vol. 134, no. 1–2, pp. 21–33, Oct. 2000, doi: 10.1016/S0167-2738(00)00710-4.
10. A. Sitka, W. Jodkowski, P. Szulc, D. Smykowski, and B. Szumiło, "Study of the Properties and Particulate Matter Content of the Gas from the Innovative Pilot-Scale Gasification Installation with Integrated Ceramic Filter," *Energies 2021, Vol. 14, Page 7476*, vol. 14, no. 22, p. 7476, Nov. 2021, doi: 10.3390/EN14227476.
11. A. Giuffrida, M. C. Romano, and G. Lozza, "Efficiency enhancement in IGCC power plants with air-blown gasification and hot gas clean-up," *Energy*, vol. 53, pp. 221–229, May 2013, doi: 10.1016/J.ENERGY.2013.02.007.
12. E. I. Koytsoumpa, K. Atsonios, K. D. Panopoulos, S. Karellas, E. Kakaras, and J. Karl, "Modelling and assessment of acid gas removal processes in coal-derived SNG production," *Appl Therm Eng*, vol. 74, pp. 128–135, Jan. 2015, doi: 10.1016/J.APPLTHERMALENG.2014.02.026.
13. A. Akachuku *et al.*, "Experimental and kinetic study of the catalytic desorption of CO2 from CO2-loaded monoethanolamine (MEA) and blended monoethanolamine – Methyl-diethanolamine (MEA-MDEA) solutions," *Energy*, vol. 179, pp. 475–489, Jul. 2019, doi: 10.1016/J.ENERGY.2019.04.174.
14. W. H. Chen, S. M. Chen, and C. I. Hung, "Carbon dioxide capture by single droplet using Selexol, Rectisol and water as absorbents: A theoretical approach," *Appl Energy*, vol. 111, pp. 731–741, Nov. 2013, doi: 10.1016/J.APENERGY.2013.05.051.
15. A. Wilk, L. Więcław-Solny, A. Tatarczuk, A. Krótki, T. Spietz, and T. Chwoła, "Solvent selection for CO2 capture from gases with high carbon dioxide concentration," *Korean Journal of Chemical Engineering 2017 34:8*, vol. 34, no. 8, pp. 2275–2283, Jun. 2017, doi: 10.1007/S11814-017-0118-X.
16. D. A. Dalrymple, T. W. Trofe, and J. M. Evans, "Liquid redox sulfur recovery options, costs, and environmental considerations," *Environmental Progress*, vol. 8, no. 4, pp. 217–222, Nov. 1989, doi: 10.1002/EP.3300080412.
17. M. A. Habib *et al.*, "A review of recent developments in carbon capture utilizing oxy-fuel combustion in conventional and ion transport membrane systems," *Int J Energy Res*, vol. 35, no. 9, pp. 741–764, Jul. 2011, doi: 10.1002/ER.1798.